Simulation of Two Compact Antipodal Vivaldi Antennas With Radiation Characteristics Enhancement

Qiancheng Ying, Wenbin Dou
State Key Laboratory of Millimeter Waves, Southeast University, Nanjing 210096, People's Republic of China
Email: seuyqc@163.com; njdouwb@163.com

***Abstract*—In this paper, two compact antipodal Vivaldi antennas (AVA) with improved Radiation Characteristics are presented. U-typed tapered slot edge (U-TSE) AVA and comb-shaped AVA with U-TSE are simulated and optimized. The -10-dB reflection coefficient bandwidth of comb-shaped AVA spans from 2.3 GHz to 18 GHz (7.83:1) and covers 15.7 GHz, while the bandwidth of conventional AVA which has the same dimensions spans from 3.3 GHz to 18 GHz (5.45:1) and covers 14.7 GHz. The U-TSE structure has the capacity to extend the low-end bandwidth limitation and improve the radiation characteristics in the lower frequencies. Compared with the conventional AVA, this modification can miniaturize the electrical size of the AVA antenna about 30%. The results regarding return loss, far field pattern, antenna gain and axial ratio are illustrated.**

I. INTRODUCTION

With the development of modern communication technology in both military and civil applications, the demand for compact, smart, wideband, and multifunctional antennas increases. The tapered slot antenna (TSA), which is still one of the most widely used wideband antennas, has a history of more than 30 years. The first TSA was introduced by Gibson [1] with exponential profile in 1979, which is also known as the ETSA or Vivaldi antenna. Vivaldi antenna is widely investigated and applied in satellite communication, remote sensing, and radio telescopes due to its broad bandwidth, low cross-polarization, and high directivity [2-4]. However, the operating bandwidth of conventional Vivaldi antenna is usually limited. First, the high-end working band is restricted by the transition structure from the microstrip to slotline. In the low-end working band, on the other hand, the bandwidth is limited by the width of the antenna patch.

In order to overcome the limitation, Gazit proposed the antipodal Vivaldi antenna (AVA) [5] in 1988. The antipodal Vivaldi antenna separates the patches with the substrate and centers them. The antenna is fed by a standard microstrip transmission line. A microstrip-to-symmetric-double-sided-slotline transition that has extremely wide operating band is employed instead of the conventional microstrip-to-slotline transition. In recent years, although many researches [6-8] on AVA have been down, how to decrease low-end cutoff frequency limited by the antenna aperture while improving the antenna radiation characteristics is still a problem. In [9], the tapered slot edge (TSE) structure is first proposed to reduce the low-end cutoff frequency while keeping the dimensions of the antenna unchanged.

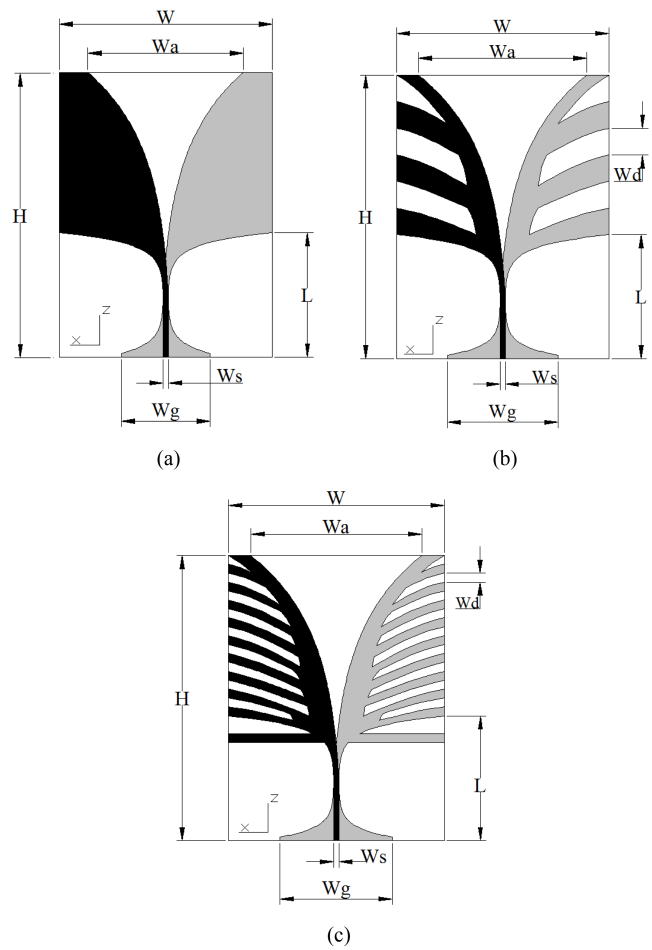

Fig. 1. Proposed evolution of the AVA configuration. (a) Conventional AVA. (b) U-TSE AVA. (c) Comb-shaped AVA with U-TSE.

In this paper, U-type tapered slot edge (U-TSE) structure is proposed. Novel U-TSE AVA and comb-shaped AVA with U-TSE are designed. By using U-TSE, the low-end cutoff frequency of the antenna shows significant reduction, indicating that the electrical size of the antenna can be miniaturized. Also, U-TSE structure can improve the antenna's radiation characteristics, such as antenna gain and axial ratio. The Ansoft simulation software high-frequency structure simulator (HFSS) [10] is used to optimize the design. Good return loss and radiation pattern characteristics are obtained in the frequency band of interest.

II. Antenna Design and Configuration

Two proposed antipodal Vivaldi antennas fed by a 50Ω microstrip transmission line are illustrated in Fig. 1(b) and (c), which are printed on the FR4 substrate of thickness 0.6 mm, relatively permittivity 4.4 and loss tangent 0.02. A 50Ω microstrip feed line has a metal strip of width Ws =1.18 mm. The inner and outer edge tapered curves of the antenna are defined as

$$x = c_1 \cdot e^{Rz} + c_2 \tag{1}$$

Where R is the opening rate. The opening rates of the inner and outer edge tapers are 0.06 and 0.4, respectively. c_1 and c_2 are determined by the coordinates of the first and last points of the exponential curve.

$$c_1 = \frac{x_2 - x_1}{e^{Rz_2} - e^{Rz_1}} \tag{2}$$

$$c_2 = \frac{x_1 e^{Rz_2} - x_2 e^{Rz_1}}{e^{Rz_2} - e^{Rz_1}} \tag{3}$$

Fig. 1 shows the evolution of the AVA configuration. First, the conventional AVA illustrated in Fig. 1(a) is designed. Then, Fig. 1(b) shows the primary modified structure. Two pairs of symmetrical U-type tapered slots are etched on the fins inspired by the tapered slot edge structure in [9], which was used to reduce the electrical size of antenna. As the U-TSE structure has a coordinate profile with the radiation fins, the comb-shaped AVA shown in Fig. 1(c) is proposed by increasing the number of U-type tapered slots. This modification is expected to further lengthen the overall effective electrical length and improve the performance of the antenna. The parameters of the proposed antennas are studied by changing one parameter at a time and fixing the others. The optimal dimensions of the proposed AVA antennas are specified in Table I.

TABLE I

The Optimal Dimensions of the Proposed AVA Antennas

	Conventional AVA	U-TSE AVA	Comb-shaped AVA
W(mm)	48	48	48
H(mm)	64	64	64
Wa(mm)	35	38	38
L(mm)	28	28	28
Wg(mm)	20	25	25
Wd(mm)	-	6	2

III. Results and Discussion

A. Return Loss

Fig. 2 illustrates the return loss curves of conventional AVA, U-TSE AVA, and comb-shaped AVA, respectively.

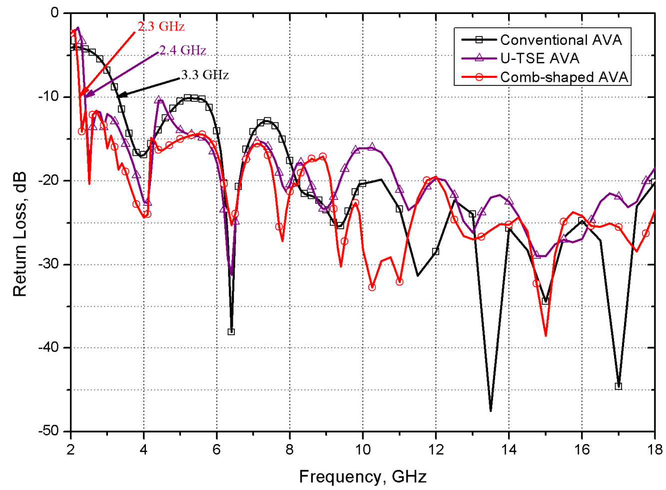

Fig. 2. Simulated return loss of the proposed AVA antennas

As shown in the figure, the low-end cutoff frequency of the conventional AVA for $S_{11} \leq$-10 dB is 3.3 GHz, while the U-TSE AVA extends it to 2.4 GHz. The comb-shaped AVA further extends the low-end cutoff frequency to 2.3 GHz and has ultra-wideband performance spanning from 2.3 to more than 18 GHz. Additional resonant points can be observed around the lower limitation of working band in both U-TSE and comb-shaped AVA. The dimensions of the conventional AVA are 48×64 mm^2, which is approximately 0.53λ× 0.7λ, where λ is the wavelength of 3.3 GHz. Also, the dimensions of the comb-shaped AVA are 48 × 64 mm^2, which is approximately 0.37λ× 0.49λ, where λ is the wavelength of 2.3 GHz. It is demonstrated that the U-TSE structure has the capacity to miniaturize the electrical size of the antenna. Although the low-end cutoff frequencies of U-TSE AVA and comb-shaped AVA are almost the same, the return loss of comb-shaped AVA is better than U-TSE AVA in the frequency band of interest, especially in the higher frequencies.

B. Current Distributions

In order to further understand the behavior of the U-TSE structure, especially in the lower frequencies, current distribution patterns of conventional AVA, U-TSE AVA, and comb-shaped AVA at 2.4 GHz are given in Fig. 3.

As the figure reveals, the surface current of the conventional AVA in region A is very small at 2.4 GHz. It is demonstrated that most of the input energy is reflected and can not be radiated. Thus, the return loss of the conventional AVA shown in Fig. 2 is very bad from 2.3 GHz to 3.3 GHz. On the other hand, by etching the U-type tapered slots, significant currents are observed in both region B and region C, indicating that the effective length of the current path on the antenna is lengthened through the modification. Besides, compared with U-TSE AVA, there are more U-type tapered slots etched on the fins of comb-shaped AVA. The effective length of the current path should be further lengthened. This is the reason why the comb-shaped AVA has the lowest cutoff frequency and the best return loss.

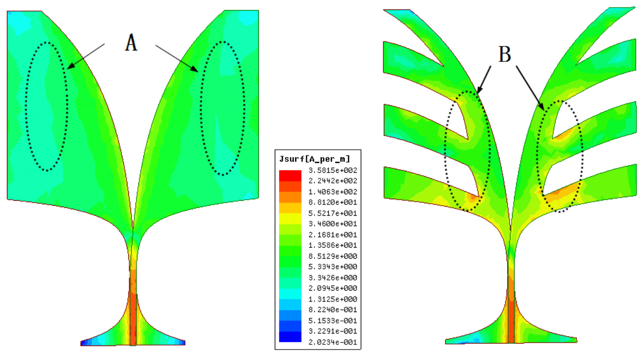

(a) (b) (c)

Fig. 3. Surface current distribution of the proposed antennas.(a) Conventional AVA. (b) U-TSE AVA. (c) Comb-shaped AVA.

C. *Radiation Patterns*

Fig. 4 illustrates simulated far-field E-plane (x-z plane) and H-plane (y-z plane) radiation patterns of the proposed AVA antennas at 4.4, 8.4, 13.5 and 17.5 GHz, including the co-polarization and cross-polarization.

As the figure shows, the proposed AVA antennas have endfire characteristics with the main lobe in the axial direction of the tapered slotline (z-direction in Fig. 1). At all four frequency points, the radiation patterns of the comb-shaped AVA show significant improvement in side lobe level and front to back ratio compared with the conventional one. The cross polarization levels are very small for all the simulated patterns and a co-pol/cross-pol ratio of better than 20 dB is observed in the direction of z-axis. Besides, the proposed antennas have symmetrical H-plane radiation pattern, while the E-plane has the slight asymmetry.

D. *Antenna Gain and Axial Ratio*

The realized gain variation with frequency of conventional AVA, U-TSE AVA, and comb-shaped AVA in the direction of z-axis is illustrated in Fig. 5.

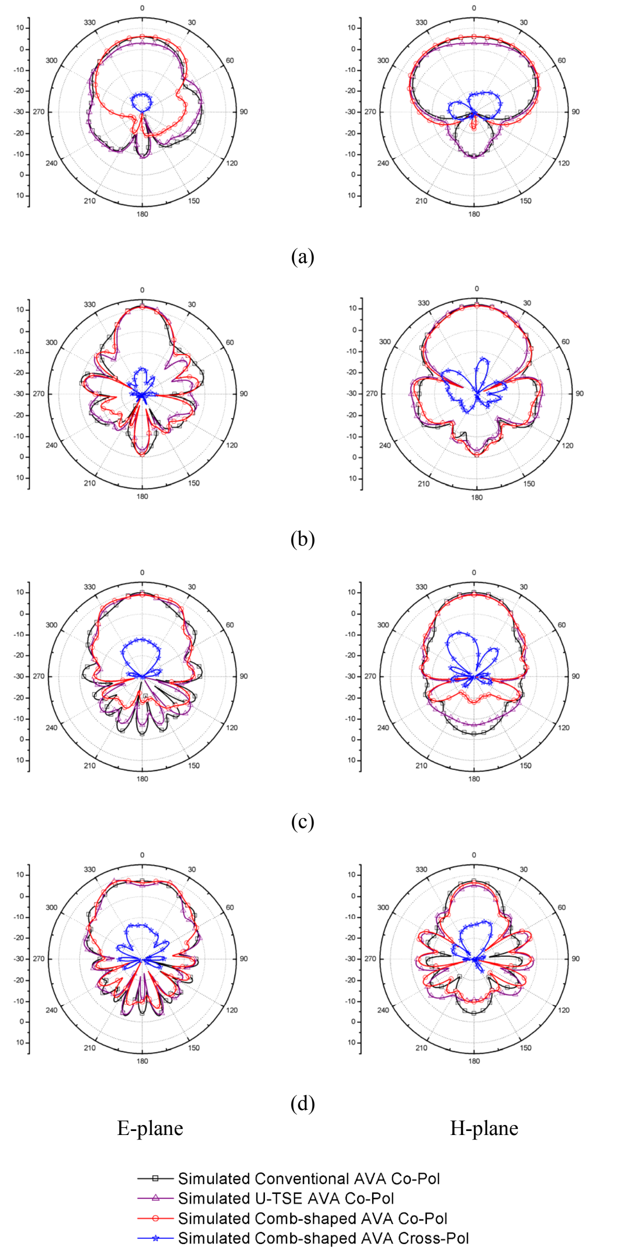

Fig. 4. E-plane (x-z) and H-plane (y-z) radiation patterns of the proposed AVA antennas at (a) 4.4, (b) 8.4, (c) 13.5, and (d) 17.5 GHz.

As shown in the figure, in the band from 2.3 GHz to 10 GHz, especially from 2.3 GHz to 6 GHz, the realized gain curves of both U-TSE AVA and comb-shaped AVA show great improvement. The minimum gain of comb-shaped AVA is at the frequency 5.7 GHz with a value about 4.4 dB and maximum gain at 8.8 GHz with a value about 11.5 dB. However, in the band after 10 GHz, the realized gain becomes worse. It is indicated that the dielectric loss is larger in the high frequencies compared with the conventional one. The reason is possibly that the longer effective length of current path on the U-TSE and comb-shaped AVA antennas causes more loss in the high frequencies.

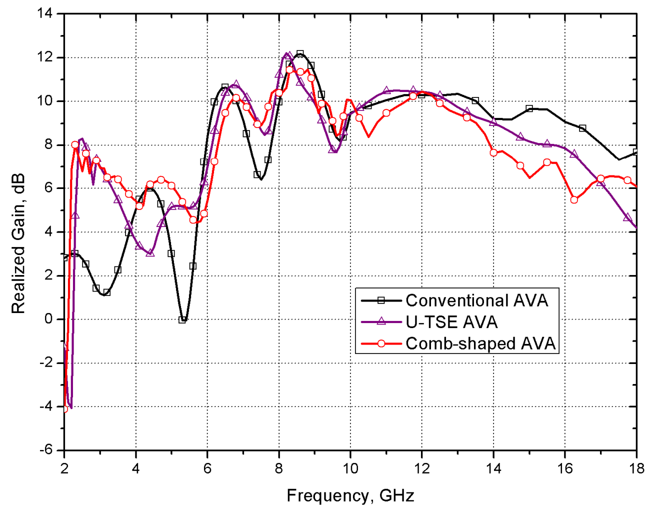

Fig. 5. Variation of the realized gain with frequency of the proposed AVA antennas.

Another parameter of the proposed AVA antennas for polarization application, the Axial Ratio variation with frequency in the z-axis direction, is shown in Fig. 7.

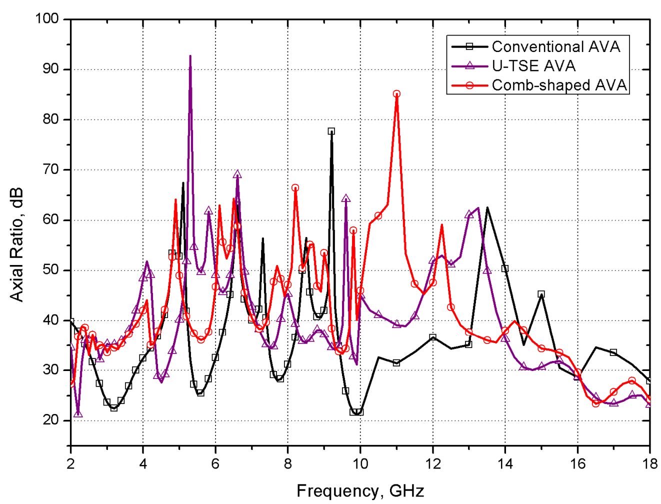

Fig. 7. Variation of the axial ratio with frequency of the proposed AVA antennas.

As the figure reveals, in the band from 2.3 GHz to 14 GHz, the axial ratio (AR) curves of both U-TSE AVA and comb-shaped AVA show significant improvement. The minimum AR of comb-shaped AVA is at the frequency 2.5 GHz with a value about 33.1 dB. It is demonstrated that U-TSE structure can help enhance the co-pol/cross-pol ratio, indicating excellent polarization purity. However, in the higher frequencies, the axial Ratio decreases because the effective thickness of the dielectric substrate increases.

IV. Conclusion

In this paper, two novel antipodal Vivaldi antennas with U-type tapered slot edge modification are proposed. With return loss better than -10 dB, the impedance bandwidth of U-TSE AVA spans from 2.4 GHz to 18 GHz, while the bandwidth of comb-shaped AVA is over the frequency range of 2.3 GHz to 18 GHz (7.83:1). The best low-end cutoff frequency for $S_{11} \leq -10$ dB is extended to 2.3 GHz from the conventional AVA 3.3 GHz. This modification can miniaturize the electrical size of the antenna about 30%. Moreover, U-TSE AVA and comb-shaped AVA behave better radiation characteristics compared with the conventional one. Simulated results show that two modified AVA antennas could be a good candidate for ultra-wideband communication systems. The implementation and measurement of the proposed antenna can be carried out in the future.

Acknowledgment

The authors gratefully acknowledge the students and teachers of State key laboratory of Millimeter Waves, for their helpful comments.

References

[1] P. J. Gibson, "The Vivaldi aerial," in *Proc. 9th Eur. Microw. Conf.*, Brighton, U. K., Jun. 1979, pp. 101-105.

[2] R. Janaswamy, D. H. Schaubert, "Analysis of the Tapered slot antenna," *IEEE Trans. Antennas Propag.*, vol. 35, no. 9, pp. 1058-1065, Sept 1987.

[3] K. S. Yngvesson, T. L. Korzeniowski, Y. Kim, and E. L. Kollberg, "The tapered slot antenna-A new integrated element for millimeter-wave application," *IEEE Trans. Microw. Theory Tech.*, vol. 37, pp. 365-374, Feb. 1989.

[4] H. Oraizi and S. Jam, "Optimum Design of Tapered Slot Antenna Profile," *IEEE Trans. Antennas Propag.,* vol. 51, no. 8, pp. 1987-1995, 2003.

[5] E. Gazit, "Improved design of the Vialdi antenna," *Proc. Inst. Elect. Eng. H,* vol 135, no. 2, pp. 89-92, Apr. 1988.

[6] A. Z. Hood, T. Karacolak, and E. Topsakal, "A Small Antipodal Vivaldi Antenna for Ultrawide-band Applications," *IEEE Antennas Wireless Propag. Lett.*, vol. 7, pp. 656-660, 2008.

[7] X. D. Zhuge, A. Yarovoy, Leo P. Ligthart, "Circularly Tapered Antipodal Vivaldi Antenna for Array-Based Ultra-wideband Near-Field Imaging," *Proc. 6th Eur Radar Conf.,* Rome, Italy, Sept. 2009, pp. 250-253.

[8] Y. X. Che, K. Li, X. Y. Hou, and W. M. Tian, "Simulation of A Small Sized Antipodal Vivaldi Antenna for UWB Applications," *ICUWB.,* Nanjing, China, Sept. 2010, pp. 1-3.

[9] P. Fei, Y.C. Jiao, W. Hu, and F. S. Zhang, "A Miniaturized Antipodal Vivaldi Antenna With Improved Radiation Characteristics," *IEEE Antennas Wireless Propag. Lett.*, vol. 10, pp. 127-130, 2011.

[10] Ansoft Corporation, Ansoft High Frequency Structure Simulation (HFSS), Ver. 13, Ansoft Corporation, Pittsburgh, PA, USA, 2010.